Nanoscale Res Lett (2010) 5:1585–1589
DOI 10.1007/s11671-010-9680-4

NANO EXPRESS

Synthesis of Heterogeneous $Li_4Ti_5O_{12}$ Nanostructured Anodes with Long-Term Cycle Stability

Duk Kyu Lee · Hyun-Woo Shim · Jae Sul An · Chin Moo Cho · In-Sun Cho · Kug Sun Hong · Dong-Wan Kim

Received: 26 April 2010 / Accepted: 29 June 2010 / Published online: 21 July 2010

Abstract The 0D-1D Lithium titanate ($Li_4Ti_5O_{12}$) heterogeneous nanostructures were synthesized through the solvothermal reaction using lithium hydroxide monohydrate ($Li(OH)\cdot H_2O$) and protonated trititanate ($H_2Ti_3O_7$) nanowires as the templates in an ethanol/water mixed solvent with subsequent heat treatment. A scanning electron microscope (SEM) and a high resolution transmission electron microscope (HRTEM) were used to reveal that the $Li_4Ti_5O_{12}$ powders had 0D-1D heterogeneous nanostructures with nanoparticles (0D) on the surface of wires (1D). The composition of the mixed solvents and the volume ratio of ethanol modulated the primary particle size of the $Li_4Ti_5O_{12}$ nanoparticles. The $Li_4Ti_5O_{12}$ heterogeneous nanostructures exhibited good capacity retention of 125 mAh/g after 500 cycles at 1C and a superior high-rate performance of 114 mAh/g at 20C.

Keywords $Li_4Ti_5O_{12}$ · Nanowires · Solvothermal reaction · Capacity retention · Li ion batteries

D. K. Lee · J. S. An · C. M. Cho · I.-S. Cho · K. S. Hong (✉)
Department of Materials Science & Engineering, College of Engineering, Seoul National University, Shillim-dong, San 56-1, Gwanak-gu, Seoul 151-744, Korea
e-mail: kshongss@plaza.snu.ac.kr

D. K. Lee
Ceramic Research & Development Division, Dongil Technology Ltd, #215-6, Bukyang-dong, Hwasung 445-854, Korea

H.-W. Shim · D.-W. Kim (✉)
Department of Materials Science & Engineering, Ajou University, San 5, Woncheon-dong, Yeongtong-gu, Suwon 443-749, Korea
e-mail: dwkim@ajou.ac.kr

Introduction

To date, the preparation of inorganic nanostructures with controlled shape, composition, and desired functions has been explored for the application to biomedicine, catalysts, and energy storages [1–3]. $Li_4Ti_5O_{12}$ has attracted attention as a Li ion battery electrode for energy storage because of its merit as zero-strain lithium insertion hosts and its stable insertion potential at 1.55 V vs. Li [4]. Many researchers have studied the synthesis of $Li_4Ti_5O_{12}$ with various nanostructures, including nanowires [5–7], nanotubes [8], flower-like nanosheets [9], and hollow-spheres [10]. These powders exhibited good electrochemical properties compared to the bulk $Li_4Ti_5O_{12}$ powder because of the shorter Li ion diffusion distances. In a wet chemical reaction, the change in the dielectric constant of the solvent can alter the thermodynamics of the reaction system and the nucleation kinetics, which modulate the particle size and size distribution of the resulting particles [11, 12].

In this work, 0D-1D $Li_4Ti_5O_{12}$ heterogeneous nanostructures were via a solvothermal reaction using $Li(OH)_2\cdot H_2O$ and $H_2Ti_3O_7$ nanowires as the templates in an ethanol/water mixed solvent at 180°C with subsequent heat treatment. The effects of the volume ratio of ethanol to water on the morphologies of the prepared $Li_4Ti_5O_{12}$ were examined with respect to the dielectric constant of the mixed solvent. Additionally, the electrochemical performances of the prepared $Li_4Ti_5O_{12}$ as an anode for Li ion batteries were evaluated and discussed with regard to the morphology of $Li_4Ti_5O_{12}$.

Experimental procedures

$H_2Ti_3O_7$ (HTO) precursors were synthesized using a hydrothermal treatment in an alkaline environment, which

was a well-known solution technique for the preparation of HTO nanowires [13]. First, 1 g of commercial anatase powder (Sigma–Aldrich, USA) was dispersed in 200 ml of a 10 M NaOH aqueous solution. The solution was stirred for 1 h at room temperature to ensure homogeneity, and then the suspension was transferred into a Teflon-lined stainless steel autoclave for the hydrothermal treatment. The autoclave was maintained at 180°C for 24 h. After the hydrothermal treatment, the suspension was centrifuged, and a white sodium titanate ($Na_2Ti_3O_7$) precipitate was obtained. Then, the precipitate was washed and dried. The prepared precipitate was soaked in a 0.1 M HCl aqueous solution for 24 h at room temperature, which fully induced cation exchange between the sodium ions and the hydrogen ions. Finally, HTO nanowires were obtained after the suspension was washed with deionized water several times and dried in a freeze dryer for 48 h.

Lithium titanate ($Li_4Ti_5O_{12}$) was synthesized using a solvothermal reaction and subsequent calcination. Lithium hydroxide monohydrate ($Li(OH)_2{\cdot}H_2O$) and the HTO nanowires were dissolved in an ethanol/water mixed solvent and autoclaved at 180°C for various reaction times (1–24 h). The volume percentage (vol.%) of ethanol to distilled water was varied from 0 to 100%, and the molar ratio of Li^+ to Ti^{4+} was 1.05. After each reaction was completed, the obtained products were washed with distilled water and ethanol. Then, the powders were dried in a freeze dryer for 48 h and finally calcined at 500 and 700°C for 2 h.

The crystal structures of the powders were analyzed using an X-ray diffractometer (M18XHF-SRA, MAC Science Co., Japan) and Raman spectroscopy (model T64000, Horiba Jovin Yvon, France). The morphologies and microstructures of the as-prepared powders were observed using a scanning electron microscope (SEM, JSM-6330F, JEOL) and a high resolution transmission electron microscope (HRTEM, JEM-3000F, JEOL).

The working electrodes were prepared as pellets with a diameter of 10 mm by pressing and punching the mixture that was composed of 60 wt% active materials, 20 wt% Super P carbon black, and 20 wt% Kynar 2801 binder. The Swagelok-type cells were assembled using the pellets as the positive electrode, a Li metal foil as the negative electrode, and a Celgard 2400 separator [14]. All of the components were immersed in an electrolyte solution of 1 M $LiPF_6$ that was dissolved in a mixture of ethylene carbonate (EC) and dimethyl carbonate (DMC) with the volume ratio of EC/DMC = 1:1.

The electrochemical properties of the assembled cells were measured using a battery cycler (WBCS 3000, WonATech, Korea). The charge/discharge tests were galvanostatically carried out between 2.5 and 1.0 V for 500 cycles at a current rate of 1C, and additionally, the cycling performance was evaluated at various rates of 1C, 5C, 10C, and 20C, in order to determine the highest rate performance.

Results and discussions

Figure 1a shows the XRD patterns of the powders that were calcined at 500°C after the solvothermal reaction in various mixed solvents, including ethanol 20 vol.% (LT-E2), 40 vol.% (LT-E4), 60 vol.% (LT-E6), and 80 vol.% (LT-E8), using the $H_2Ti_3O_7$ nanowire and $Li(OH)_2{\cdot}H_2O$. When the amount of ethanol was more than 60 vol.%, pure $Li_4Ti_5O_{12}$ was well crystallized without a secondary phase and indexed to cubic spinel $Li_4Ti_5O_{12}$ (JCPDS Card #: 49-0207). Figure 1b–e show the representative SEM images of the powders that were prepared in various solvents. After the solvothermal reaction and the calcination, the powders retained their wire-like morphology, and interestingly, LT-E6 and LT-E8 exhibited a 0D-1D heterogeneous nanostructures with nanoparticles (0D) on the surface of the wires (1D), which was confirmed in Fig. 2.

Figure 2a, b, and c represent the TEM images of LT-E4, LT-E6, and LT-E8, respectively. The surface of LT-E4 was smooth without any nanoparticles, whereas LT-E6 and LT-E8 had tetrahedral nanoparticles on the surface. More interestingly, the particle size of LT-E6 was much larger than

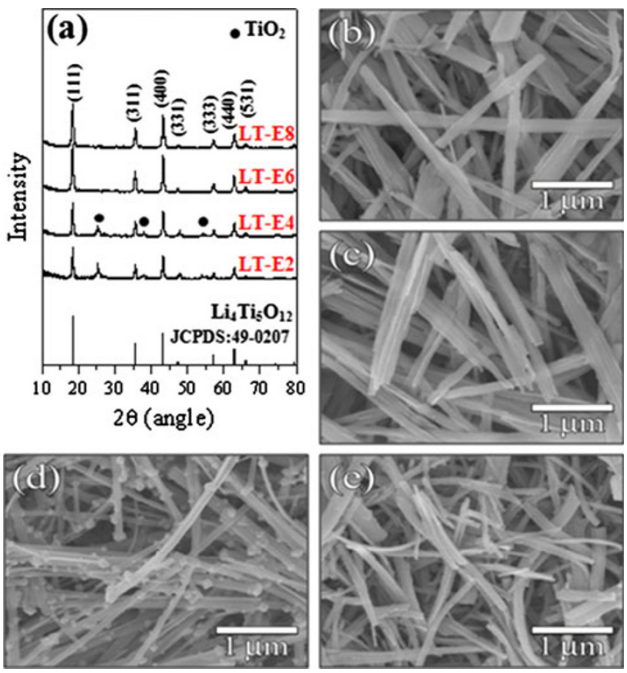

Fig. 1 **a** XRD patterns of the powders calcined at 500°C after the solvothermal reaction in various mixed solvents. Typical SEM images of **b** LT-E2, **c** LT-E4, **d** LT-E6, and **e** LT-E8 powders calcined at 500°C

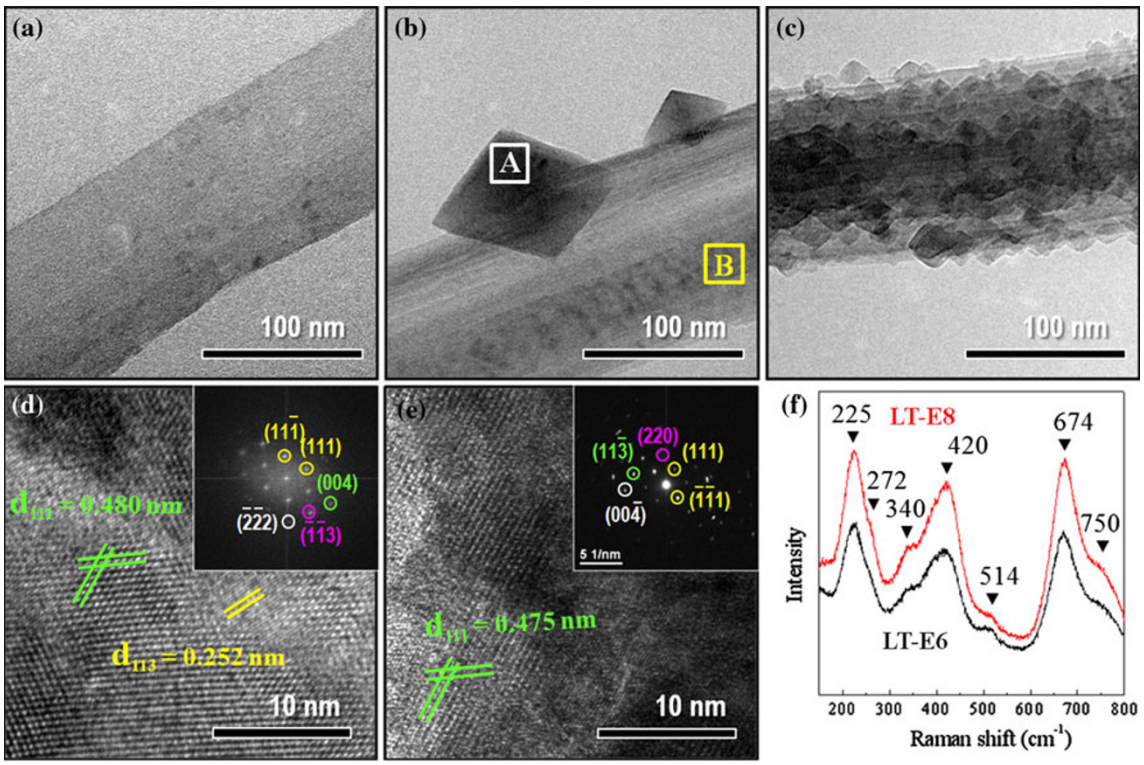

Fig. 2 TEM images of **a** LT-E4, **b** LT-E6, **c** LT-E8 powders calcined at 500°C, respectively. **d** and **e** HRTEM images of A and B regions in the (**b**), respectively. Insets in **d** and **e** show the corresponding FFT and SAED patterns, respectively. **f** Raman spectra of the LT-E6 and LT-E8 powders

that of LT-E8. This is attributed to the low dielectric constant (ε) of the mixed solvent ($\varepsilon_{water} = 80$, $\varepsilon_{EtOH} = 25$) [15].

In principle, a solvent with a low dielectric constant is easier to reach higher supersaturation, which can accelerate the nucleation rate. As well, the radius of the nuclei decreases with the reduction of the ε of the solvent from the electrostatic model using the following relationships [16]. Therefore, both the dielectric constant and the primary particle sizes of the powders that were generated in the mixed solvent decreased with increasing ethanol concentration. Figure 2d and e represent the HRTEM images of the A and B regions in the Fig. 2b. The measured interplanar distances in both A and B regions closely matched the lattice spacings of $Li_4Ti_5O_{12}$. The corresponding fast Fourier transform (FFT) and selected area electron diffraction (SAED) patterns (the insets in Fig. 2d and e) also confirm that both the polyhedral particles and the wires are of the same phase $Li_4Ti_5O_{12}$. Single phase of $Li_4Ti_5O_{12}$ was investigated by Raman spectroscopy. As shown in Fig. 3f, vibration peaks were observed at 225, 272, 340, 420, 514, 674, and 750 cm^{-1},

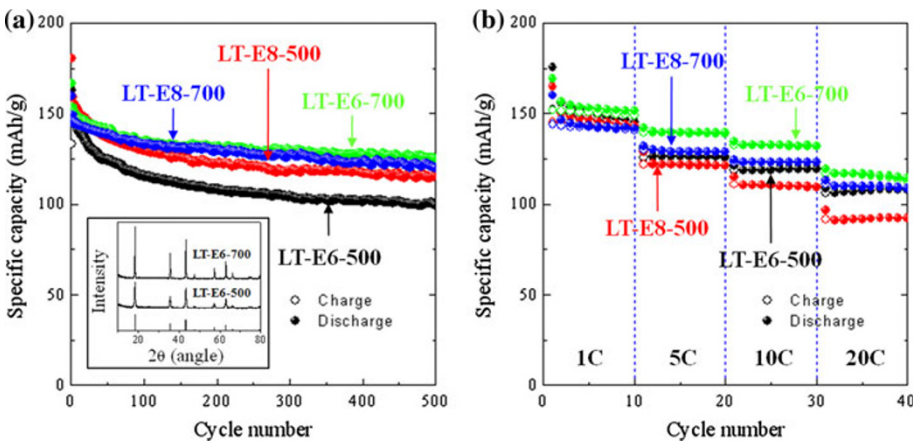

Fig. 3 **a** Variation of the discharge–charge specific capacities versus the cycle number and **b** cycling behavior at different C rates for the LT-E6-500, LT-E6-700, LT-E8-500, and LT-E8-700 powders, respectively. Inset in **a** shows the XRD patterns of the LT-E6-500 and LT-E6-700 powders

consistent with the spectra that were reported for the $Li_4Ti_5O_{12}$ [17]. These observations demonstrate the formation of phase-pure $Li_4Ti_5O_{12}$.

Although further experimental observations are needed for the exact mechanism, the formation mechanism of the 0D-1D $Li_4Ti_5O_{12}$ in this study can be proposed as follows. In the early stage of the reaction, the Li^+ species (or intermediate derivatives of lithium metals) in the solution reacted with the HTO nanowires that were locally dissolved at the interface and in situ precipitated to 0D $Li_4Ti_5O_{12}$ nanoparticles. The similar nucleation process was reported in the formation of multiple $NaNbO_3/Nb_2O_5$ heterostructure nanotubes [18]. This process was possible even at a low temperature, ~180°C, because of the easier supersaturation caused by the lowered dielectric constant of the mixed solvent. The propagation of the reaction was expected to occur from the front of the HTO to the interior until the entire HTO wires were transformed into $Li_4Ti_5O_{12}$ through reaction with barium ions that diffused during the growth of the outer $Li_4Ti_5O_{12}$ nanoparticles, finally yielding the phase-pure 0D–1D $Li_4Ti_5O_{12}$ nanostructures.

Figure 3 represents the charge–discharge behavior of heterogeneous $Li_4Ti_5O_{12}$ nanostructures calcined at 500°C (LT-E6-500, LT-E8-500) and 700°C (LT-E6-700, LT-E8-700). LT-E6-700 was also single phase $Li_4Ti_5O_{12}$ such as LT-E6-500 (inset in Fig. 3a). Both LT-E6-500 and LT-E6-700 exhibited almost the same capacities (150 mAh/g) in the early stages. After 500 cycles, the capacity of LT-E6-700 was 125 mAh/g, whereas the capacity of LT-E6-500 was 100 mAh/g, which was attributed to the high crystallinity of LT-E6-700 by the calcination at a high temperature [19]. For comparison in our work, TiO_2 nanowire (1D) samples were also prepared by the calcinations of $H_2Ti_3O_7$ nanowires at same temperature, 700°C. Although $Li_4Ti_5O_{12}$ and TiO_2 had similar theoretical capacities (~170 mAh/g), $Li_4Ti_5O_{12}$ nanowires exhibited much higher capacities and long-term cyclabilities than TiO_2 nanowires, which might originate from the larger specific surface area (BET surface areas of 40 and 15 m^2/g for $Li_4Ti_5O_{12}$ and TiO_2, respectively) that resulted from the heterogeneous nanostructures. It has been also reported that excellent electrochemical performance could be achieved in high surface area anodes such as V_2O_5–SnO_2 double-shelled nanocapsules and porous Co_3O_4 nanocapsules due to efficient Li ion and electron transport [20, 21]. However, up until now, this long-life performance of 500 cycles in $Li_4Ti_5O_{12}$ has not been reported.

Figure 3b shows the rate capability of LT-E6-500, LT-E8-500, LT-E6-700, and LT-E8-700 while examining rates of up to 20C. The cells were charged and discharged at 1C for the first 10 cycles, and then the rate was increased in stages to 20C. The heterogeneous LT-E6-700 nanowires exhibited a slightly better capacity at high rates than LT-E6-500. A specific discharge capacity of LT-E6-700 after 10 cycles at 1C was 151 mAh/g. This value gradually decreased as the rates increased. However, at a high rate of 20C, the specific discharge capacity was still 114 mAh/g, which was about 75% of the capacity at 1C.

Conclusion

The heterogeneous $Li_4Ti_5O_{12}$ nanostructures were synthesized via the solvothermal reaction in an ethanol/water mixed solvent with subsequent calcination at 500–700°C. The heterogeneous nucleation of the $Li_4Ti_5O_{12}$ nanocrystals was induced, and the size of the nanoparticles on the surface of the wire was modified by changing the dielectric constant of the solvent during the solvothermal reaction.

The heterogeneous 0D-1D $Li_4Ti_5O_{12}$ nanostructures calcined at 700°C exhibited a higher lithium storage capacity of 125 mAh/g after 500 cycles at 1C and a superior cycle performance (114 mAh/g) even at a high rate of 20C. The enhanced reversible capacity and cycling performance were attributed to the large surface area of the 0D-1D heterogeneous nanostructures, which enabled the use of the $Li_4Ti_5O_{12}$ nanowires as potential host materials for high-powder Li ion batteries.

Acknowledgments This research was supported by Future-based Technology Development Program (Nano Fields) through the National Research Foundation of Korea (NRF) funded by the Ministry of Education, Science and Technology (2010-0019116).

References

1. J. Liu, F. Liu, K. Gao, J. Wu, D. Xue, J. Mater. Chem. **19**, 6073 (2009)
2. J. Liu, D. Xue, Adv. Mater. **20**, 2622 (2008)
3. C. Yan, D. Xue, Adv. Mater. **20**, 1055 (2008)
4. S. Scharner, W. Weppner, P. Schmid-Beurmann, J. Electrochem. Soc. **146**, 857 (1999)
5. J.R. Li, Z.L. Tang, Z.T. Ahang, J. Electrochem. Soc. **142**, 1431 (1995)
6. J. Li, Z. Tang, Z. Zhang, Electrochem. Comm. **7**, 894 (2005)
7. J. Kim, J. Cho, Electrochem Solid-state Lett. **10**, A81 (2007)
8. Y. Li, K. Xi, X.P. Gao, Mater. Lett. **63**, 304 (2009)
9. Y.F. Tang, L. Yang, Z. Qiu, J.S. Huang, Electrochem. Comm. **10**, 1513 (2008)
10. J. Huang, Z. Jiang, Elecrochem. Solid-state Lett. **11**, A116 (2008)
11. J.W. Mullin, Crystallization (Elsevier Butterworth–Heinemann, Boston 1993)
12. A.S. Myerson, Molecular Modeling Applications in Crystallization (Cambridge University Press, Cambridge, 1999)
13. Y. Wang, G. Du, H. Liu, D. Liu, S. Qin, N. Wang, C. Hu, X. Tao, J. Jiao, J. Wang, Z.L. Wang, Adv. Funct. Mater. **18**, 19 (2008)

14. D.W. Kim, Y.D. Ko, J.G. Park, B.K. Kim, Angew. Chem. Int. Ed. **46**, 6654 (2007)
15. S.M. Puranik, A.C. Kumbharkhane, S.C. Mehrotra, J. Mol. Liq. **59**, 173 (1994)
16. H.I. Chen, H.Y. Chang, Colloid Surf. A **242**, 61 (2004)
17. G. Yan, H. Fang, H. Zhao, G. Li, Y. Yang, L. Li, J. Alloys Comp. **470**, 544 (2009)
18. C. Yan, L. Nikolova, A. Dadvand, C. Harnagea, A. Sarkissian, D.F. Perepichka, D. Xue, F. Rosei, Adv. Mater. **22**, 1741 (2010)
19. Y. Li, G.L. Pan, J.W. Liu, X.P. Gao, J. Electrochem. Soc. **156**, A495 (2009)
20. J. Liu, H. Xia, D. Xue, L. Lu, J. Am. Chem. Soc. **131**, 12086 (2009)
21. J. Liu, H. Xia, L. Lu, D. Xue, J. Mater. Chem. **20**, 1506 (2010)